Electronic Supplementary Information for:

Redox and acid–base properties of asymmetric non-heme (hydr)oxo-bridged diiron complexes

Anna Jozwiuk,[a] Audrey L. Ingram,[a] Douglas R. Powell,[a] Boujemaa Moubaraki,[b] Nicholas F. Chilton,[b] Keith S. Murray[b] and Robert P. Houser*[c]

[a]Department of Chemistry & Biochemistry, University of Oklahoma, Norman, OK 73019, USA. [b]Chemistry Department, Monash University, Clayton, Victoria 3168 Australia. [c]Department of Chemistry & Biochemistry, University of Northern Colorado, Greeley, CO 80639, USA. Fax: +1 970 351 2176; Tel: +1 970 351 2877; E-mail: robert.houser@unco.edu

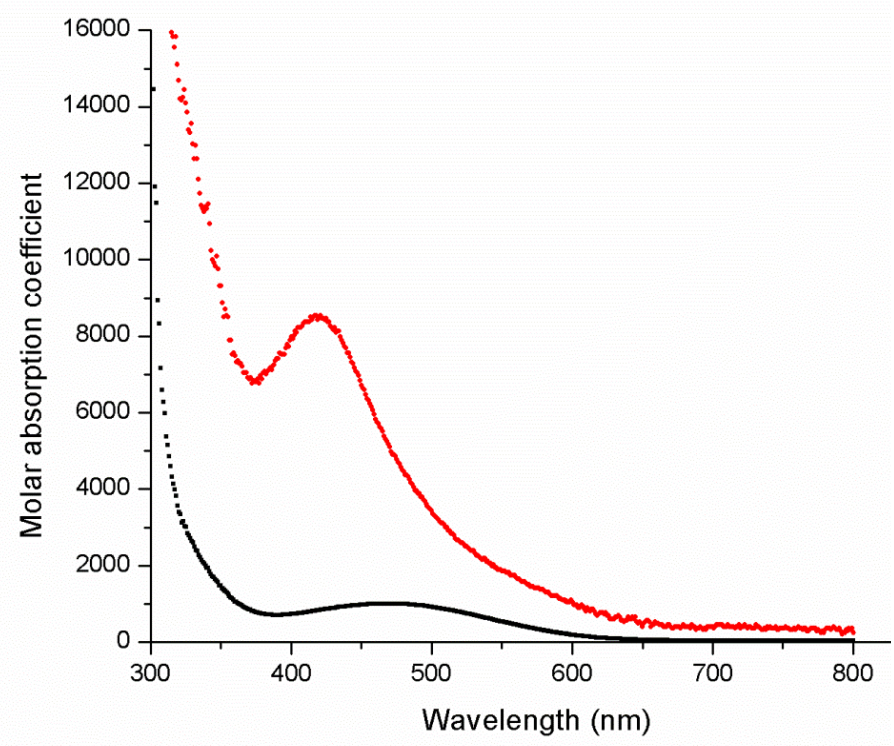

Figure S1. UV-Vis spectrum of $[(FeL)_2]$ (**4**) in MeCN (λ_{max} at 471 nm, $\varepsilon = 1000$) (black) and after exposure to air (λ_{max} at 420 nm, $\varepsilon = 8500$), (red).

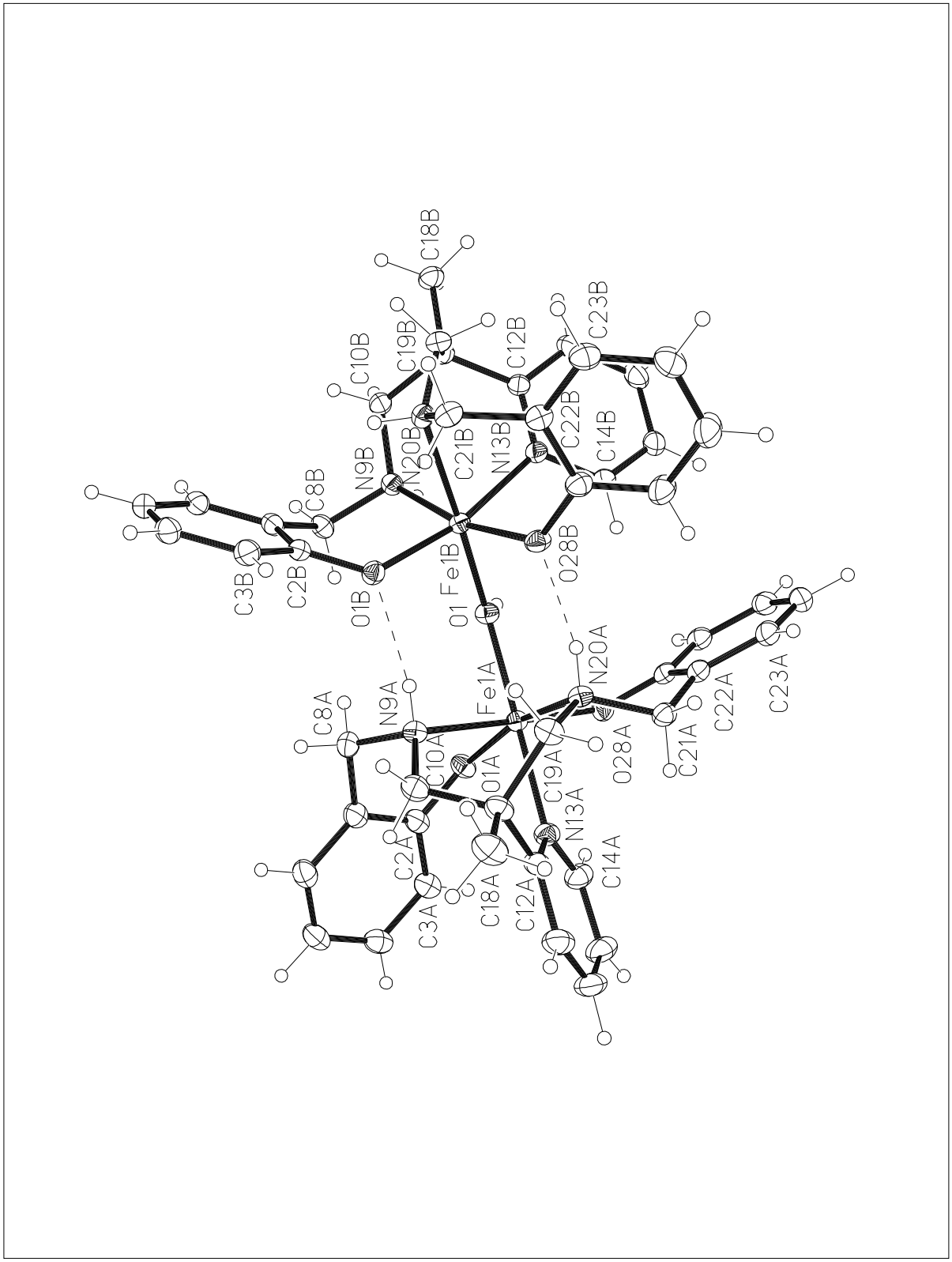

Figure S2. Representation of the X-ray structure of the cationic portion of $[(FeL)_2(\mu\text{-}OH)]BPh_4 \cdot CH_2Cl_2$ (**1**$\cdot CH_2Cl_2$).

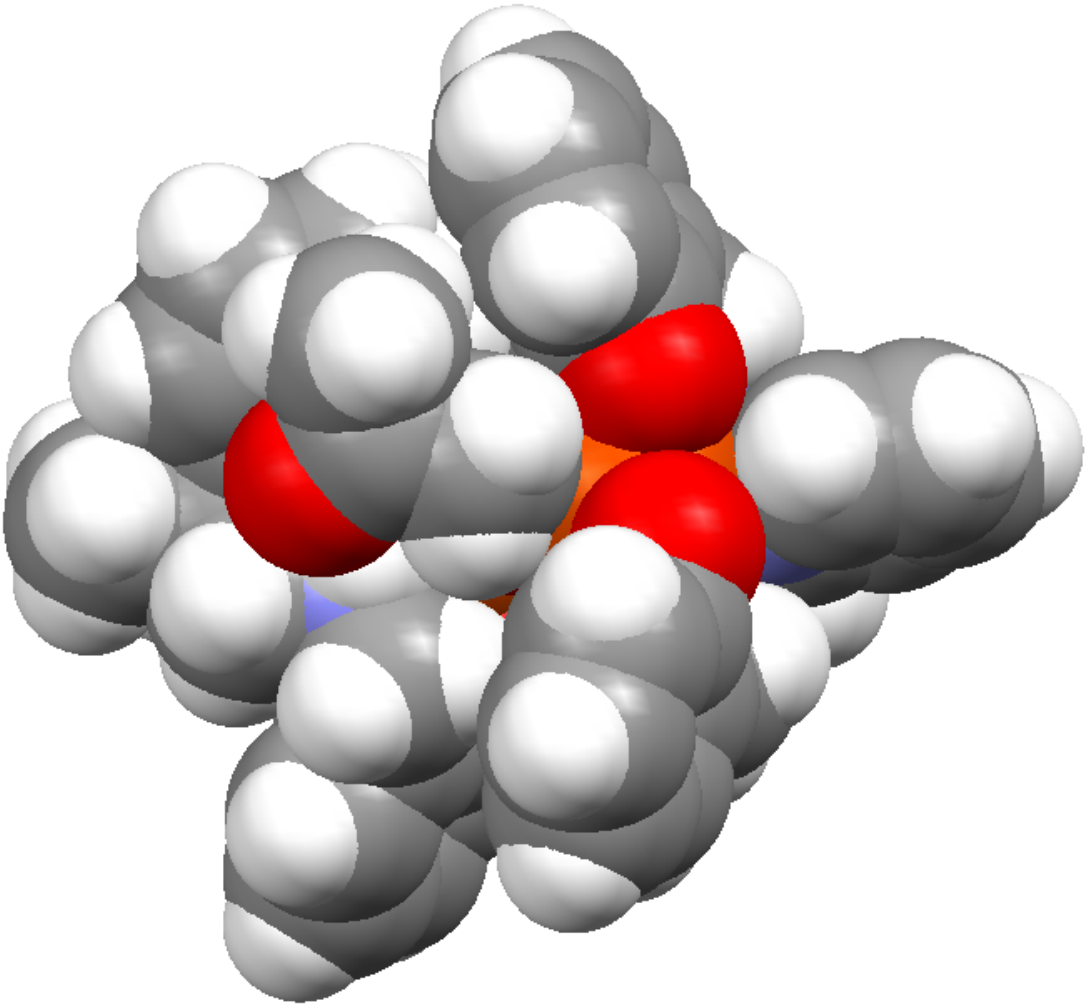

Figure S3. Space-filling representation of $[(FeL)_2(\mu\text{-}O)]\cdot(CH_3)_2CO$ (**2**$\cdot(CH_3)_2CO$).

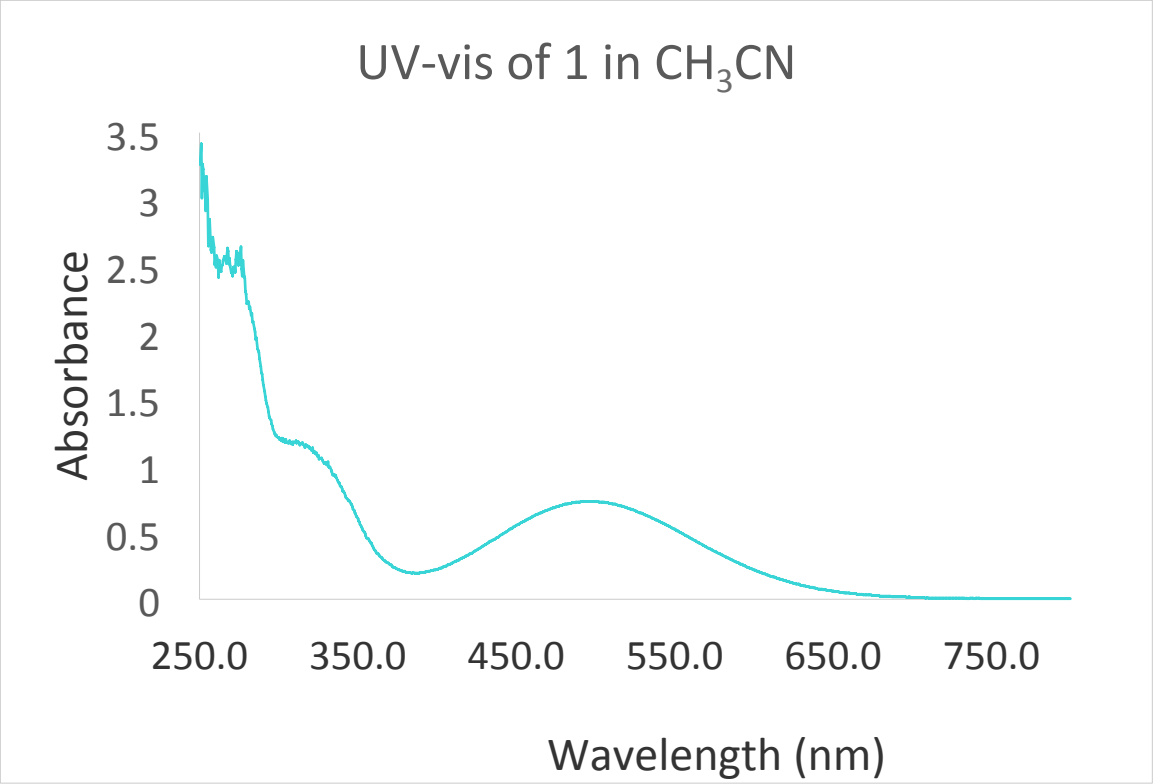

Figure S4. UV-visible spectrum of a CH_3CN solution of **1**.

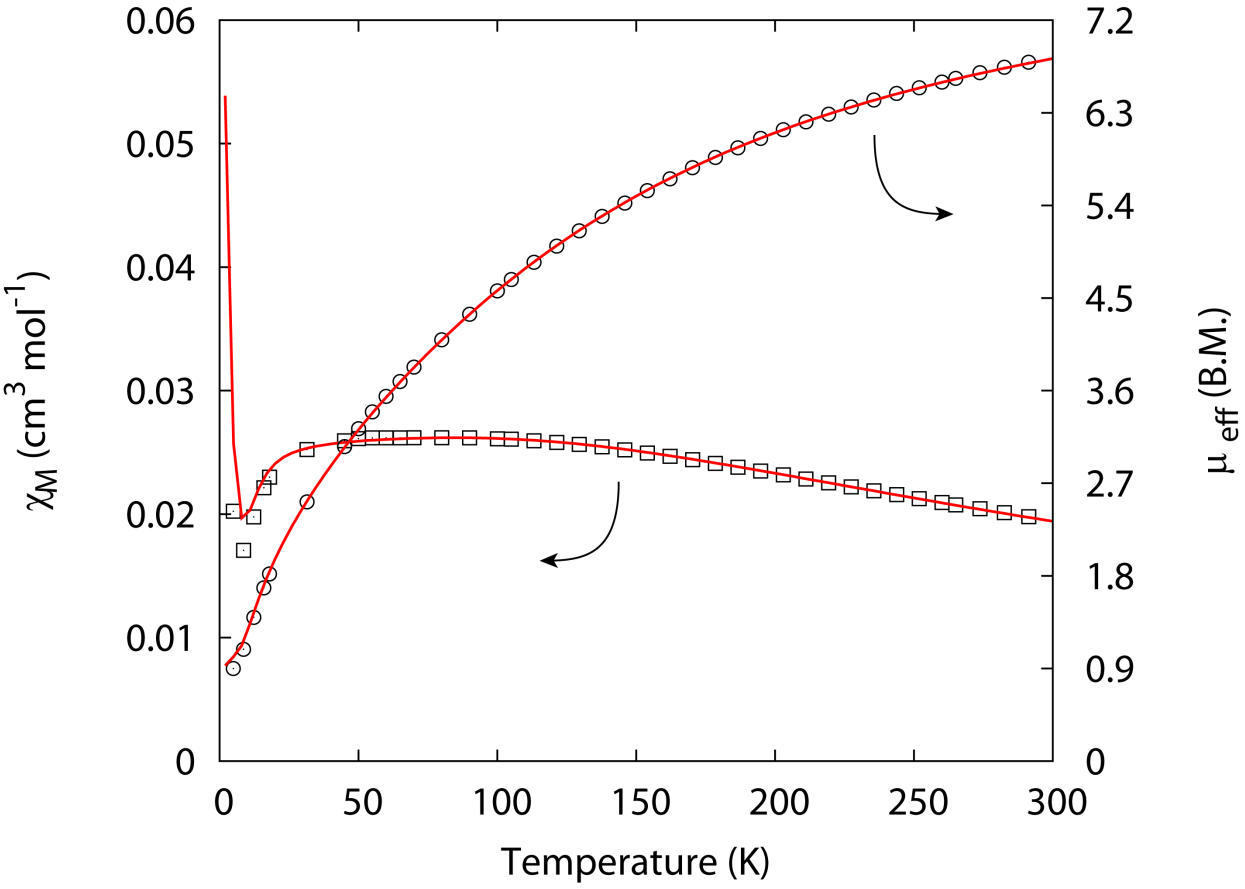

Figure S5. Plot of molar susceptibility vs. temperature for crystalline **1**·CH_2Cl_2.

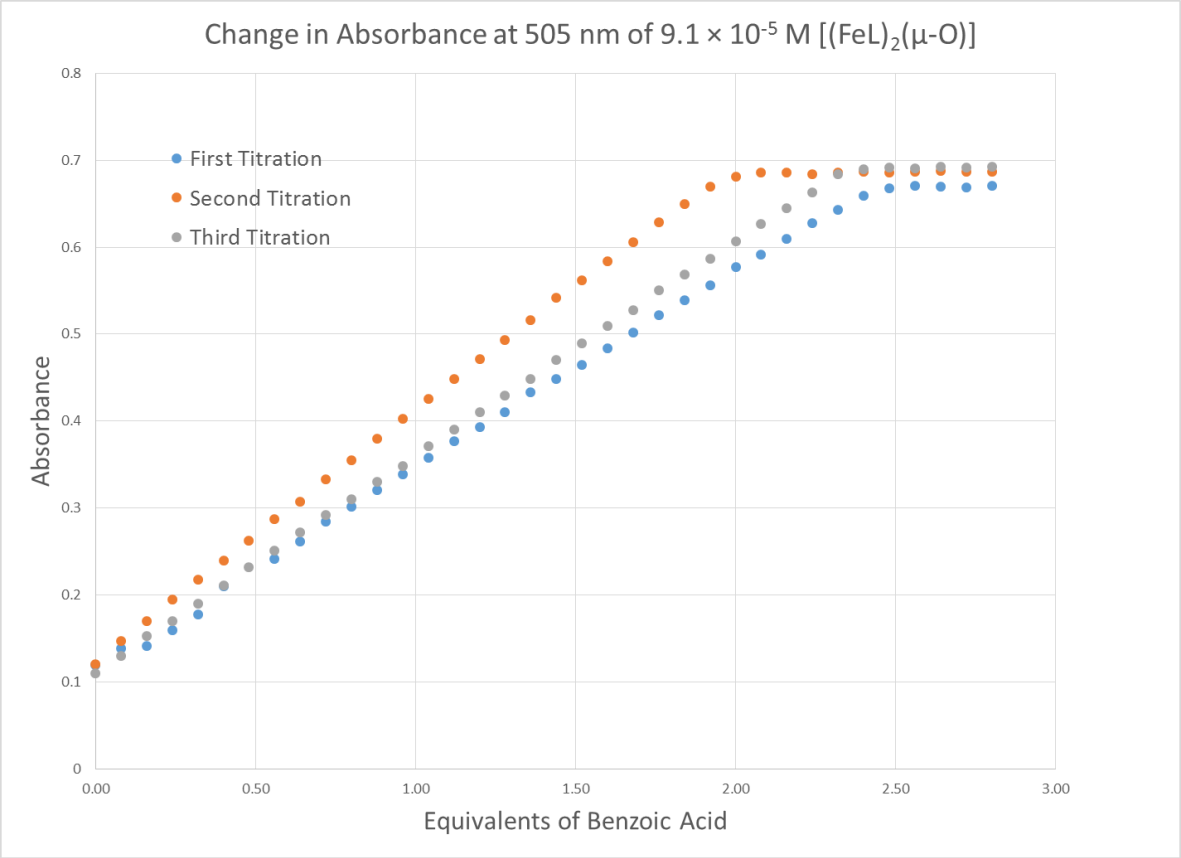

Figure S6. Change in absorbance at 505 nm of 9.1×10^{-5} M **2** with addition of benzoic acid (9.1×10^{-4} M) in acetonitrile.

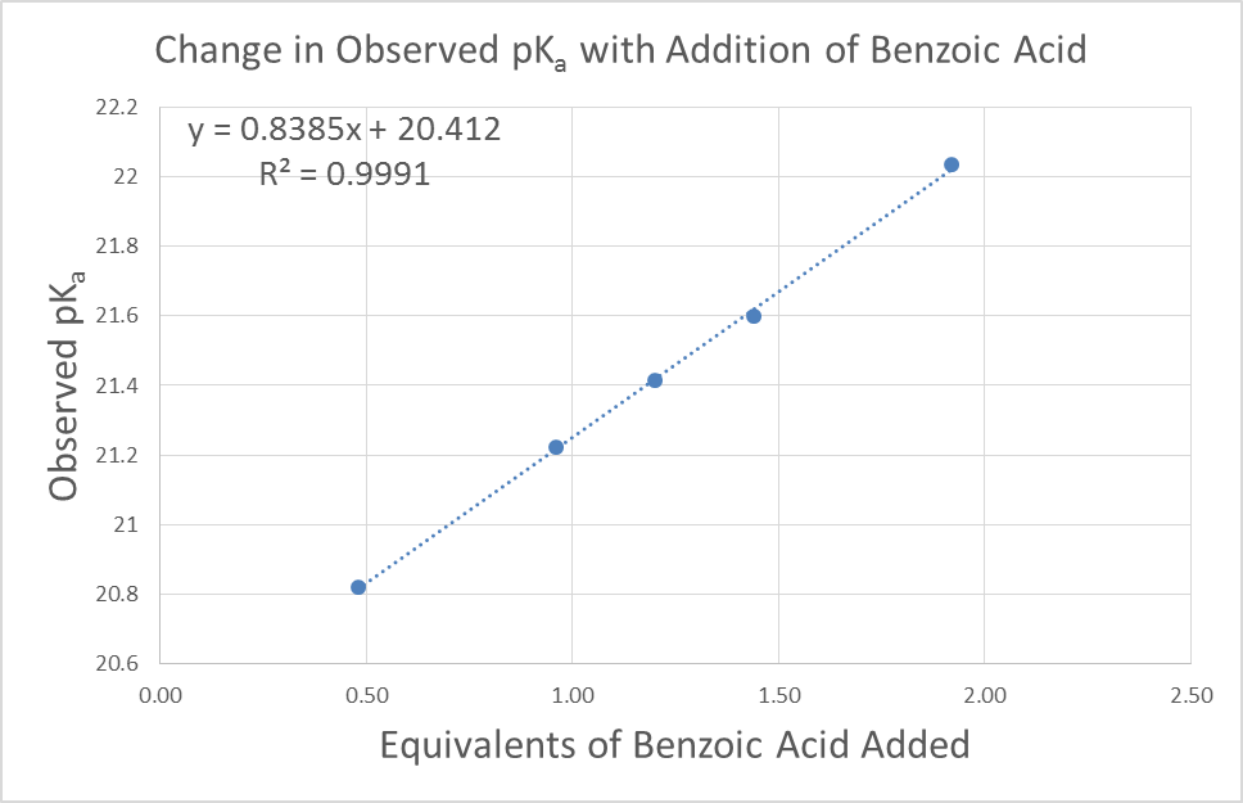

Figure S7. Change in calculated pK_a value for **2** as more equivalents of benzoic acid are added. The theoretical value if no benzoic acid were present can be estimated from the y-intercept; 20.4 in this case.

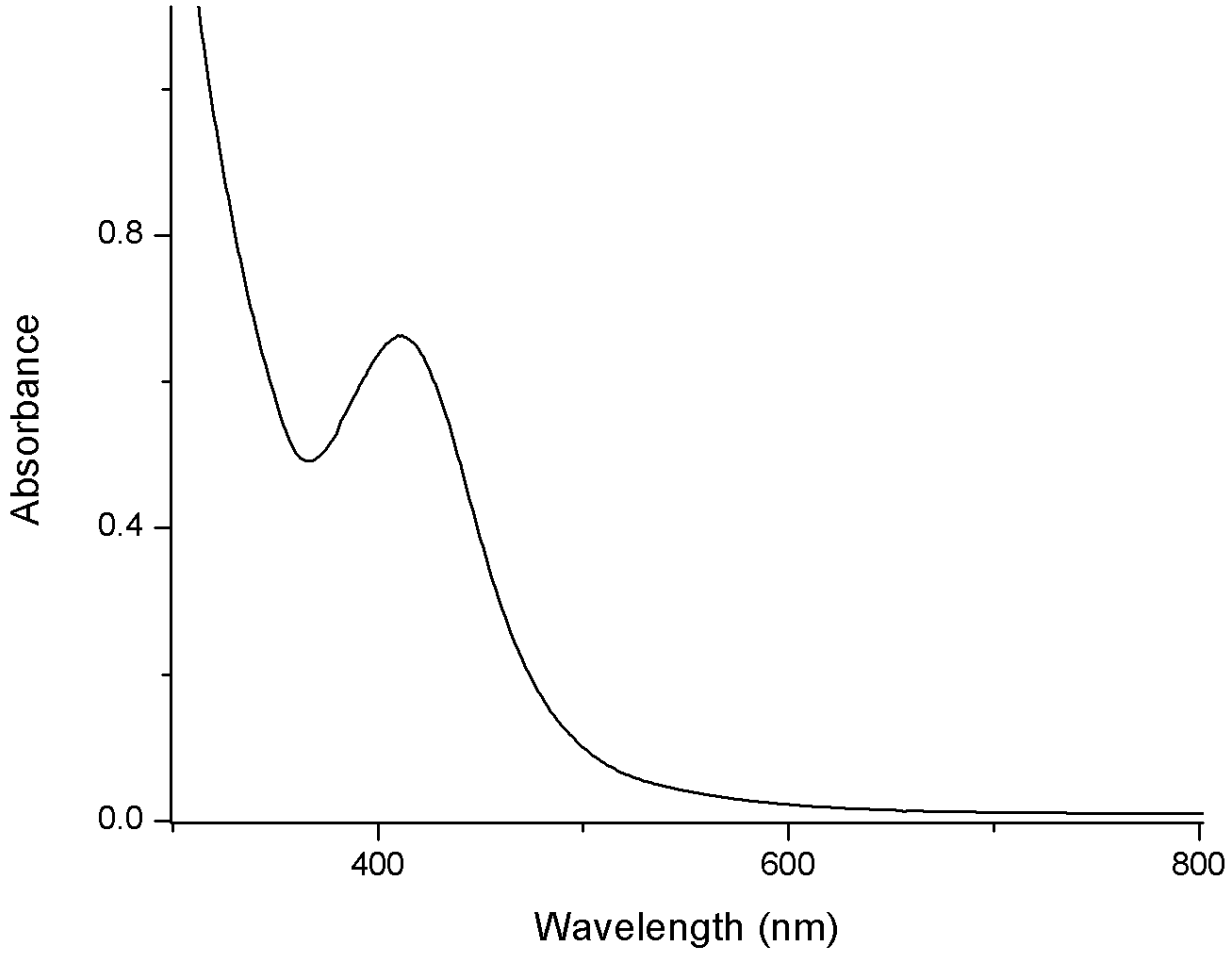

Figure S8. UV-visible spectrum of $CoCp_2BPh_4$ (0.9×10^{-3} M) in MeCN. Molar absorptivity at 412 nm = 262 $M^{-1}cm^{-1}$.

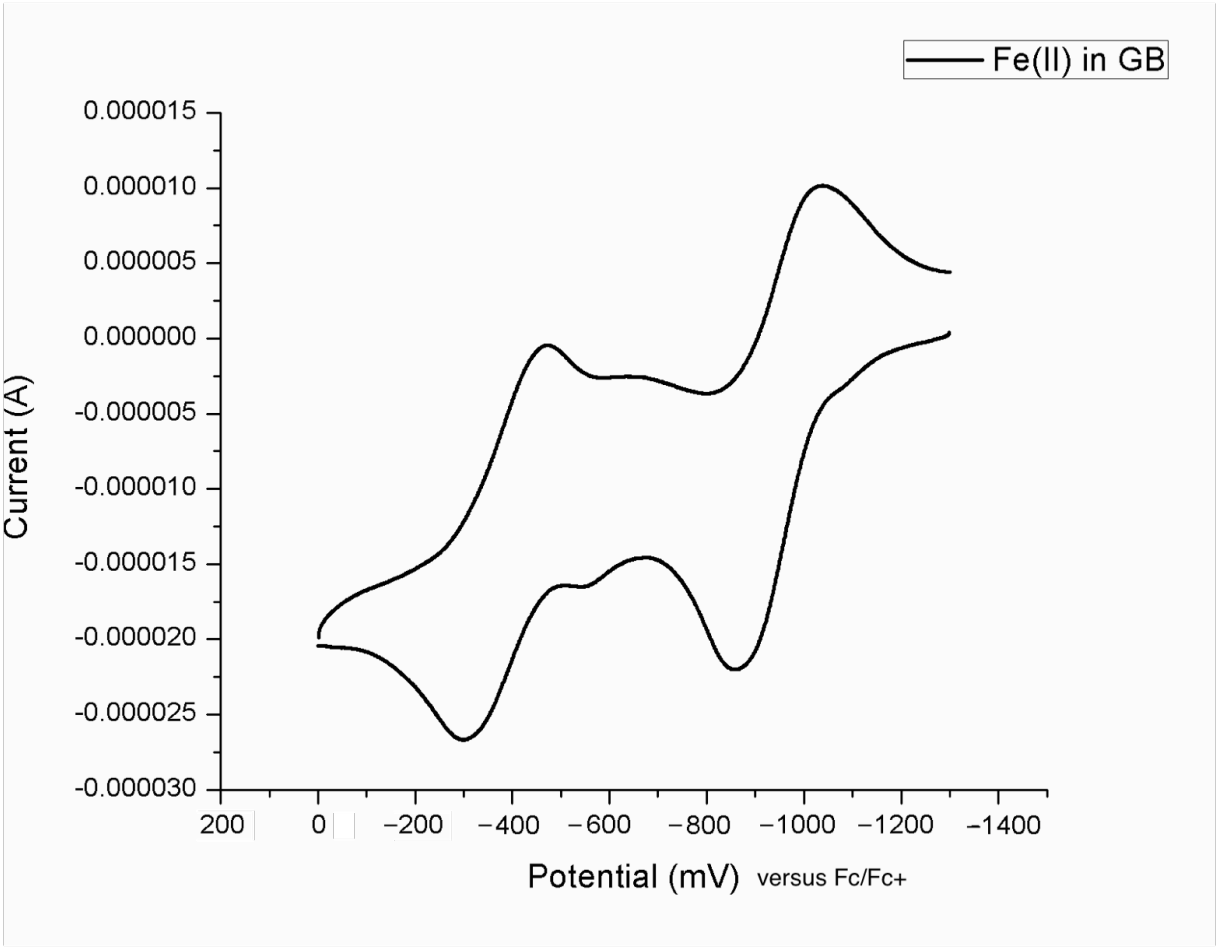

Figure S9. Cyclic voltammogram (scan rate = 100 mV s^{-1}; 0.1 M $TBAPF_6$ supporting electrolyte) of a 1 mM solution of **4** in CH_3CN.